TIME-RESOLVED VISUALIZATION OF TRANSIENT COMPRESSIBLE FLOWS

H. KLEINE [1,c]

[1] School of Engineering and Information Technology, University of New South Wales, Canberra, ACT 2600, Australia

[c] Corresponding author: Tel.: +61 2 6268 8047; Fax: +61 2 6268 8276; Email: h.kleine@adfa.edu.au

KEYWORDS:
Main subjects: high-speed photography, flow visualization
Fluid: high speed flows, compressible flows
Visualization method(s): shadow, schlieren, interferometry
Other keywords: shock waves, instability, explosions, shock interaction with obstacles

ABSTRACT During the last decade, high-speed camera technology has considerably advanced, and this has opened new possibilities for the investigation of highly transient processes. Using these new cameras together with suitable visualization techniques, it is now possible to investigate fully transient high-speed flows in unprecedented detail and quality. Earlier high-speed camera systems already had, in principle, enabled researchers to obtain time-resolved records, but most of these systems had significant shortcomings, mostly with respect to their inherent complexity. The new developments in the high-speed camera sector have removed many of these limitations, although there is a continuing need for further improvement, primarily with respect to the spatial resolution of the obtained visualization records. Most of the techniques developed for the visualization of compressible flows can be used in time-resolved mode, which allows one to show, from the records of a single experiment, how certain flow features develop. Time-resolved visualization thus contributes much to the qualitative explanation of possibly complex flow processes as detailed information on the evolution of flow features enables one to clearly distinguish between cause and consequence in a process. The records also provide quantitative information about a flow, either directly by tracking the location and/or shape of clearly distinguishable flow features in space and time, or by adequate post-processing techniques that may reveal the development of less obvious patterns within a flow. Such data would only be available from single-image visualizations, if the process in question were extremely reproducible.

This paper will outline some of the recent developments in this field, and it will discuss the potential and the limitations one encounters when using various density-sensitive visualization techniques in time-resolved mode. Several applications illustrate how this approach can reveal and explain a number of previously undetected phenomena in a variety of highly transient compressible flows. It is demonstrated that time-resolved visualization offers numerous advantages which often outweigh its shortcomings, which in most cases are related to a so far inevitable loss in spatial resolution. It is also demonstrated that time-resolved visualizations can have a significant educational value as a record of the evolution of a process is often visually more powerful than single images.

INTRODUCTION

A fully transparent medium is typically invisible to the naked eye and its movement or flow can in most cases only be seen with the help of special visualization techniques [1]. For the investigation of compressible flows, the vast majority of investigations uses so-called density-sensitive visualization methods which have become staple diagnostic tools in this area of fluid mechanics.

In addition to being invisible, many of these flow processes occur at speeds too high for human perception. The typical time constant associated with human perception is approximately 0.1 s, a consequence of visual inertia [2]. It is therefore necessary to combine an adequate visualization method with the techniques of high-speed photography to produce a visual record of the flow which then can be examined and analyzed.

The photographic technique to “freeze” rapid motion by exposing a photographic plate in a darkened room with a short light pulse was already developed in 1852 by William Henry Fox Talbot [3]. This approach has become arguably the

most enduring method of high-speed photography and is still widely used in almost all laboratories in the world that are investigating high-speed processes. Such single high-speed photographs can produce excellent and highly detailed images of a flow, but can typically only deliver a single frame of the event. Many flows of practical and academic interest are, however, inherently unsteady, that is, their shape, dimensions and properties change rapidly with time. A single snapshot of these flows, no matter how detailed, will typically only reveal a small fraction of the temporal development of the flow. A full recording of the history of the flow requires a number of such images, taken at intervals that are smaller than the relevant characteristic time of the observed process. This introduces the concept of time-resolved visualization, the main subject of this contribution, which is an extension of a previous review paper [4].

EXPERIMENTAL METHODS

Time-resolved high-speed photography and high-speed cameras

Time-resolved high-speed photography is almost as old as photography itself [3-5] and has been discussed in many publications. In the decades before electronic image recording via charge-coupled devices (CCDs), image separation was mostly obtained by opto-mechanical means: one either had to move the recording medium fast enough so that a (single) stroboscopic light source could produce multiple images on different parts of this medium, or one had to sweep a light beam rapidly over stationary film with in-between mounted stops effectively acting as shutters and image separators. A third option was to use multiple light sources arranged in an array, which generate a sequence of light pulses, each of which forms a spatially and temporally separated image of the object under investigation. These three recording schemes appear in the form of rotating drum, rotating mirror and Cranz-Schardin cameras, most of which were characterized by high cost, a relatively large physical size, and a usually high degree of complexity [4, 5]. As a consequence, time-resolved visualization was not a standard approach and only infrequently applied. Within the last ten years, CCDs have all but replaced film as recording medium, and the fact that these sensors can be gated and read out at high frequencies has removed the need for the aforementioned opto-mechanical components, and has led to new generations of high-speed cameras. The type of the recording CCD determines resolution, exposure time and frame rate: CMOS-based sensors have to be read out and "cleared" before they can record a new image, while sensors with an ISIS (In-situ Storage Image Sensor) structure, invented by Etoh and Mutoh [6, 7], have a multi-layered architecture where the images are stored in individual layers. CMOS-based cameras can typically deliver an almost arbitrarily high number of high-resolution images at lower to moderate frame rates (the number of frames is only limited by the available computer memory), but at high frame rates the resolution has to be lowered to provide enough time for the image information to be read out into memory. The ISIS architecture, in which information is not stored into memory but moved from one layer to the next, allows the CCD to record in full resolution at all frame rates, but current technology limits both the numbers of pixels as well as the number of layers and thus images. For currently available commercial high-speed cameras, the cross-over point lies at around 60,000 frames per second (fps) – at lower frame rates, CMOS-based CCDs provide better resolution and more frames, while above the threshold, the ISIS sensor has superior resolution. Most of the examples discussed in the following involve highly transient flows that require frame rates above 100,000 fps for adequate time-resolved recording and were therefore visualized with ISIS-based cameras.

While the recent advances in time-resolved high-speed imaging are truly remarkable, the general observation still holds that time-resolved recording typically sacrifices spatial resolution and therefore delivers less detailed records than a single-shot visualization. It is expected that future high-speed camera developments will increase the spatial resolution as well as the obtainable frame rates so that the existing difference in image quality is likely to be decreased.

Visualization techniques

In the present discussion, only so-called density-sensitive visualization techniques will be considered, in which a flow is made visible by recording how changes in the density of the flow affect a traversing light beam. These techniques are based on the fact that the speed of light c in a transparent medium depends on the density ρ of the medium. For gases, the dependency is expressed in the linear Gladstone-Dale equation [1]

$$n \equiv \frac{c}{c_0} = 1 - K\rho \ , \tag{1}$$

where n is the refractive index, c_0 is the speed of light in vacuum, and K is the Gladstone-Dale constant that depends on the medium and on the wavelength of the traversing light beam. The latter dependency is in most cases weak unless the frequency of the light corresponds to a resonant frequency of the medium.

A light beam that passes through areas in which the density changes leaves the path it would have traveled in the case of constant density. Therefore it reaches a recording screen placed behind the object of interest at a different location, under a different impingement angle, and after a different transit time. Each of these modifications can be optically detected and measured, and each corresponds to a unique set of measurement/visualization techniques. Displacements are captured with the shadowgraph methods, schlieren techniques detect deflections, and the methods of interferometry are used to measure phase shifts that are equivalent to transit time differences. All of these techniques have been used for scientific investigations since the second half of the 19th century and are mature diagnostic tools for experimental studies in transparent media. Extensive descriptions are given in various monographs and articles on flow visualization, e.g., [1, 8, 9].

It is a common feature of all major categories of density-sensitive visualization techniques that their basic setups are equally suitable for time-resolved operation, provided an appropriate combination of light source and high-speed camera can be implemented [4]. Time-resolved imaging only becomes difficult when special recording techniques such as holography are used, as the stringent recording requirements of these techniques are normally not met by typical high-speed cameras. The following discussion will be confined to techniques that use standard recording media. Figure 1 is a schematic of typical setups which remain essentially unchanged regardless of whether the recording is single-image or time-resolved.

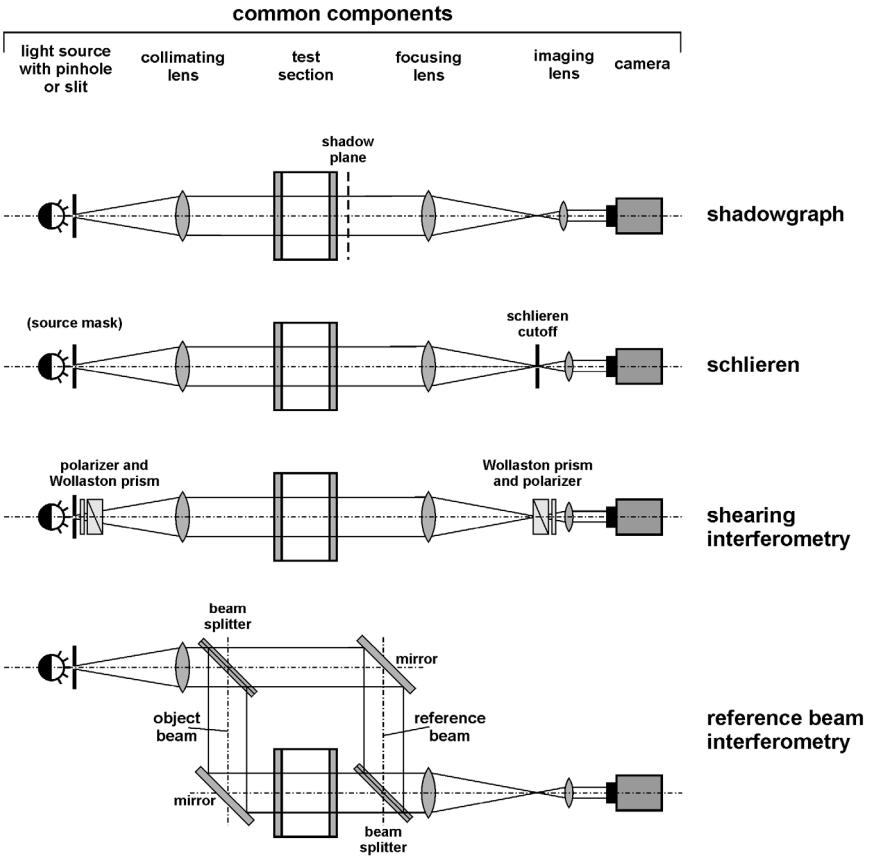

Fig. 1: Schematic of typical setups of density-sensitive visualization systems. While many variations of the basic layout exist, the setup with a parallel light beam traversing the test section is arguably the most commonly used configuration. The sketch also highlights the large degree of commonality between different density-sensitive visualization methods. (from [4])

CURRENT LIMITATIONS OF TIME-RESOLVED IMAGING

Time-resolved images typically have a lower spatial resolution than single-shot images. This implies that detecting minuscule elements of a flow field is currently still a difficult task, in spite of the additional information on the temporal evolution of such elements. An important example is the detection of the onset of irregular shock reflection in fully unsteady flow fields. For each shock Mach number in a given gas, there exists a limiting angle θ_{trans} on the reflecting surface beyond which the regular two-shock configuration of incident and reflected shock can no longer be maintained. Past this transition point, a third shock wave, the so-called Mach stem, develops. The exact experimental determination of this transition angle is still a major challenge, and theoretical and numerical predictions differ – often substantially – from experimentally obtained values. The main problem is that the Mach stem is initially extremely small and may even maintain an optically almost undetectable size for a relatively long time. The experimental detection depends strongly on the resolution of the recording medium and the chosen magnification of the visualization. Single-shot images, with their usually high resolution, may be more reliable to show the presence of the wave, but one would have to have a highly reproducible test setup to narrow down the transition point – the associated demands on reproducibility typically exceed the available control measures in existing facilities. Time-resolved records avoid, to a large extent, reproducibility issues, but may not be able to show diminutive flow elements because of their reduced image resolution. Increasing the image magnification in the visualization setup improves the situation up to the point where motion blur is of the same order of magnitude as the spatial resolution of the camera. Further details on this issue are given in [4]. It is estimated that a high-speed camera would have to have a resolution comparable to currently available SLR cameras (i.e., several megapixel) in combination with frame rates exceeding 500,000 fps and exposure times below 50 ns in order to be able to detect minuscule flow elements such as emerging Mach stems.

TIME-RESOLVED VISUALIZATION OF COMPRESSIBLE FLOWS: EXAMPLES AND APPLICATIONS

The remainder of the paper contains a number of examples which highlight various advantages of time-resolved flow visualization. Each example demonstrates the added diagnostic potential that time-resolved imaging provides. Animated versions of some of the presented examples and many other applications have recently been compiled as a DVD [10]. Such animated display of the results is a key element of time-resolved visualization as it can provide further insight into the mechanisms that shape a flow. Schardin [11] outlined that such animation was crucial because of the human ability to understand and interpret basic elements of a transient process simply by observing its motion. He argued that this additional means of analysis would be lost if one used time-resolved images only for frame-by-frame inspection and therefore advocated the use of animated display in addition to a detailed examination of individual frames. In the pre-digital age of photography, however, such a processing of time-resolved records required substantial effort and was therefore not routinely done.

TRACKING TRAJECTORIES

An obvious application of time-resolved imaging is the tracking of wavefronts or other objects as they propagate through the field of view, provided the tracked objects are large enough not to be affected by the previously outlined limitations of image resolution. For reproducible processes, this could also be achieved by evaluating a large number of individual test results, possibly with less limitations regarding image resolution. Time-resolved imaging, however, provides substantial savings in time and effort – in some shock tube applications, a single time-resolved image sequence obtained with a high-speed camera would have taken several days or even weeks to be compiled from single-shot results [4].

Time-resolved sequences have been used to determine the trajectory of blast waves– these data were then processed to obtain the overpressure-distance curve for the investigated explosive, from which the TNT equivalence factor could be determined as a function of distance from the charge [12]. An important result of these tests was that this TNT equivalence factor can vary significantly with distance and that the single values for this factor often found in the literature constitute a serious oversimplification. Figure 2 gives some sample results.

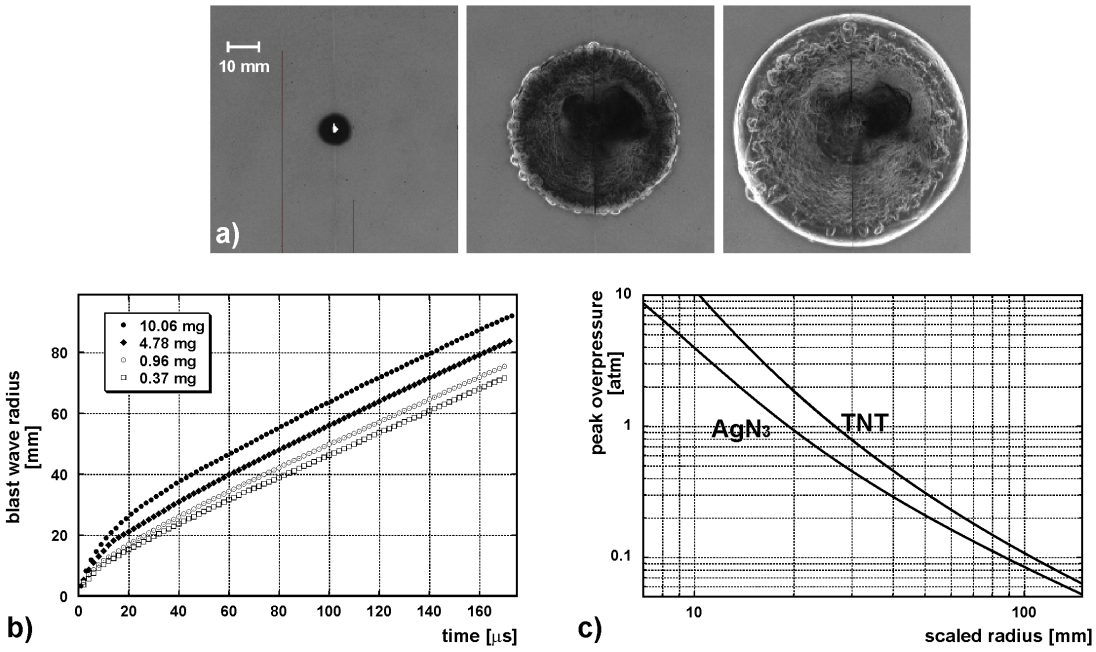

Fig. 2: (adopted from [4])
a) three frames of a time-resolved schlieren visualization of a blast wave generated by the explosion of a 10 mg AgN_3 charge (frame rate: 10^6 fps; time between shown frames: 25 μs). The charge was suspended on a thin nylon thread and ignited by a Nd:YAG laser pulse. The first frame shows the flow field at approximately 4 μs after ignition.
b) blast wave radius vs. time after ignition; data obtained from four time-resolved visualizations of explosions of charges of AgN_3 of different mass; measured from records such as Fig. 2a
c) peak hydrostatic overpressure vs. scaled distance for 1 mg charges of TNT and silver azide (obtained from curves shown in b) by applying the procedure outlined in [12]).

The results of time-resolved visualizations can also be processed to yield an *x-t* diagram of the waves [13]. These synthetic schlieren streak images can be used to highlight wave propagation patterns. In cases where the wave that is to be tracked is a prominent feature of the visualization record, the main role of such schlieren streak images is to illustrate the overall wave behaviour as detailed *x-t* data are more accurately obtained from the individual frames. In cases, however, where a wave motion may be masked by other processes in the flow, the *x-t* plot provides evidence of basic motion patterns that may be difficult to obtain directly from the individual frames. This is illustrated in Fig.3, which presents two such *x-t* diagrams, one for a blast wave, and one for the waves within a shallow open cavity in a supersonic free stream. In the latter case, a resonance process within the cavity leads to pressure oscillations that can reach sound pressure levels greatly exceeding 120 dB [14]. While pressure sensors can easily pick up these oscillations, it is difficult to track and follow the wavefronts on time-resolved visualization records as there exist multiple wave reflection processes. Some waves may become visible for a short period, as indicated in Fig. 3b, but they usually become less defined once they enter regions in which other processes occur. The processed *x-t* diagram (Fig. 3c), on the other hand, taken along a constant height along the length of the cavity, essentially filters the abundance of optical information and clearly indicates a dominant and repeated wave motion within the cavity. The speed of the main wave determined from this image corresponds well – within 1 % – to that predicted by a resonance model for these cavity flows.

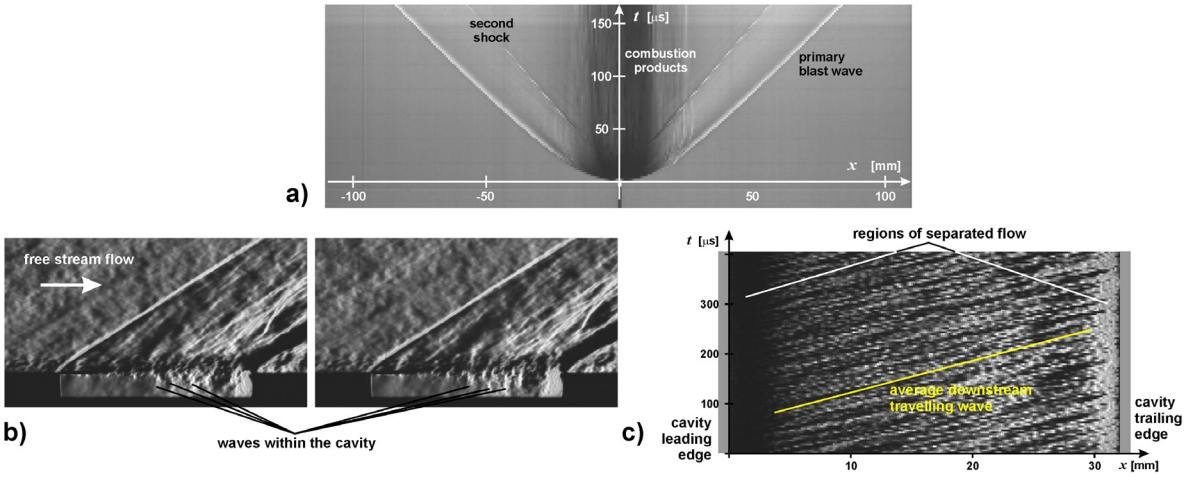

Fig. 3: a) schlieren streak record (along centreline of the explosion) obtained from time-resolved visualizations of expanding blast waves (such as Fig. 2a), here for a charge of 4.9 mg AgN_3
b) two consecutive frames from a time-resolved visualization of the flow within a shallow cavity; free stream Mach number $M = 2$, cavity length-to depth ratio $L/D = 8$; frame rate 250,000 fps, exposure time 0.5 μs
c) schlieren streak record (along the cavity length, at distance D above the cavity floor and thus immediately below the shear layer) obtained from the complete sequence of time-resolved visualizations shown in (b)

In time-resolved interferometry [15], one may not only track wavefronts but also the fringes that depict the isopycnics (lines of constant density) in the flow. As some fringes may merge or disappear from the field of view during the flow process, time-resolved information is crucial to quantify the density distribution – a single image would not contain the "history" of the fringes. This is illustrated in Fig. 4, which shows a shock wave (M_S = 1.33 in air of p_1 = 0.45 bar) passing over a circular cylinder (diameter: 20 mm). The interferometer was set to infinite fringe spacing so that in this planar flow field, each fringe corresponds to a line of constant density with a density increment of $\Delta\rho = 0.019$ kg/m^3 between two fringes. The development of the fringes indicates that the density continuously decreases from the stagnation region at the front end of the cylinder towards the incident shock. The fringes terminating in the reflected shock illustrate how the reflected shock continually loses strength towards the reflection point, which at a polar angle of approximately 45 degrees becomes the triple point of a Mach reflection.

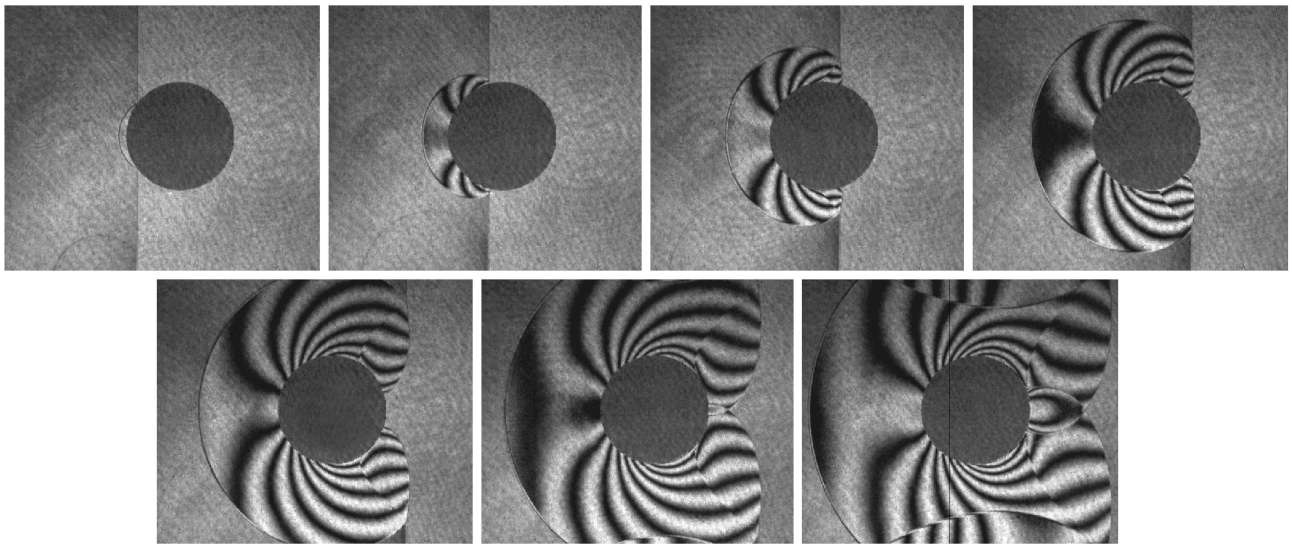

Fig. 4: Frames from a time-resolved monochrome Mach-Zehnder interferometry visualization of the interaction of a shock wave (M_S = 1.33 in air of pressure p_1 = 0.45 bar) with a circular cylinder (diameter: 20 mm); sequence taken with 330,000 fps; time between shown frames 12.1 μs

Some fringes in the stagnation region merge entirely with the reflected shock and are no longer visible at later instants. The third frame of Fig. 4 shows, for example, a system of six fringes between the front face of the cylinder and the foot of the incident shock, which represents a total density difference of 0.113 kg/m^3. The density at the front face of the cylinder has, however, as a result of the flow expanding around the cylinder, already decreased from its initial value at the first instant of interaction. The latter value can, with good accuracy, be assumed to be the value behind a normal reflected shock, which can be determined through the well-known jump relations for one-dimensional shock waves. A single interferometric record would therefore not contain sufficient information to determine the required reference value at the cylinder front face. The time-resolved sequence, however, allows one to deduce this density reference value by establishing the number of fringes that have merged with the reflected shock.

SELF-SIMILAR FLOWS

Flows that have no inherent length scale are typically described as self-similar or pseudo-steady, which means that the flow structure at any point in time is a scaled replica of the structure the flow had at an earlier instant. In gas dynamics, such flows are encountered, for example, in shock diffraction and reflection off straight surfaces. For most of these flows, self-similarity has been shown on the basis of comparing the wave patterns at different times. Time-resolved Mach-Zehnder interferometry allows one to take this a step further and to compare the density distributions at different times. Interferometric images of the density field, taken within a single test, quantitatively reveal to which extent the relative importance of various mechanisms driving and influencing a flow change with time. The sequence of polychrome interferograms of Fig. 5 clearly proves that the depicted irregular shock reflection process is self-similar within the limitations imposed by image resolution: all isopycnics can be seen from the beginning of the process and they maintain their shape throughout the reflection – viscous effects close to the wall are seen to play only a minor role.

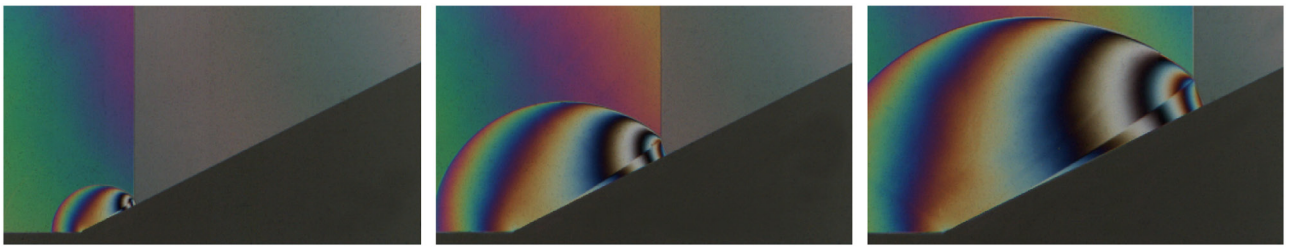

Fig. 5: Frames from a time-resolved polychrome Mach-Zehnder interferometry visualization of the reflection of a shock wave (Ms = 1.26 in air of pressure p_1 = 0.45 bar) off a 26 degree ramp; sequence taken with 330,000 fps; time between shown frames 45.6 µs

PROCESSES WITH LOW REPRODUCIBILITY

Entirely unsteady processes with initial conditions that are difficult to reproduce within reasonable limits are a formidable challenge for an experimental investigation. Time-resolved visualization gives one the opportunity to obtain sufficiently detailed results in a single experiment, which would be nearly impossible to reconstruct from single images taken in different experiments. Typical examples for such applications include processes with instabilities or other random elements. The example briefly described below outlines the interaction of a transonic projectile with a gaseous plume [16]. This test series was conducted to qualitatively investigate the ability of transonic aircraft in ground effect to extinguish fires. The obvious experimental difficulty is to fire the projectile at precisely the same speed and the same height above ground and to hit the gaseous plume at the same position. As seen below, this process is highly transient, and the high sensitivity of some flow features like the bow shock stand-off distance on the Mach number of the projectile makes it unlikely that this process could be faithfully reproduced from multiple experiments.

Figure 6a shows a projectile passing through a helium plume. The projectile has a Mach number of M = 1.06 and a clearance above the ground plate of h = 3.5 d where d is the projectile diameter. The bow shock of the projectile curves forward towards the wall and does not generate a reflected wave [17] but then disperses from the instant that it passes

through the helium column. This is an indication of the varying sound speed of the gas ahead of the projectile. The bow shock becomes a well-defined discontinuity again about 75 μs after the interaction has started. During this time, the stand-off distance of the bow shock to the tip of the projectile initially increases by almost 35% before returning to its original value prior to the interaction. The projectile itself is seen piercing through the gaseous column and the rapid acceleration of the helium displaced by the projectile creates a near-spherical disturbance that moves away from the projectile tip to eventually catch up with leading bow shock. All other flow features around the projectile – the expansion zones at the base of the projectile and at the junction of the ogive forebody and the cylindrical part as well as recompression shock and its reflection – pass through the helium column with only minimal distortion. As with the bow shock, a slight dispersion visible as loss of definition of the wave fronts is observed, which indicates the presence of a medium with a varying speed of sound. The effect of this dispersion is also seen on pressure traces that were obtained 30 mm upstream and downstream of the helium column. In absence of the helium flow, both traces are virtually identical, but the dispersion introduced by the gaseous column leads to a 25% widening of the positive phase for the signal of the downstream sensor (Fig. 6b).

The gaseous column is initially moved downstream by the bow shock, with a maximum displacement of approximately one column diameter (third frame in Fig. 6a). The duration of the displacement of the helium column is about 36 μs and is finished before the expansion zones of the projectile cross the foot of the column. These waves shift the helium column back to its original position where it encounters the recompression shock and its reflection from the ground. This second shock interaction has, however, little effect on the overall displacement of the helium column and appears to primarily introduce additional disturbances at the pipe outlet in the ground surface. For the remainder of the observation time, these disturbances slowly grow as do those higher up in the column, which are generated by the projectile itself and subsequently by the interaction of the wake with the column. The overall structure of the column appears, however, to remain largely unaffected, at least within the limited observation time. Tests conducted with a higher projectile Mach number (M = 1.16) show qualitatively a similar behavior, and no significant increase of the displacement.

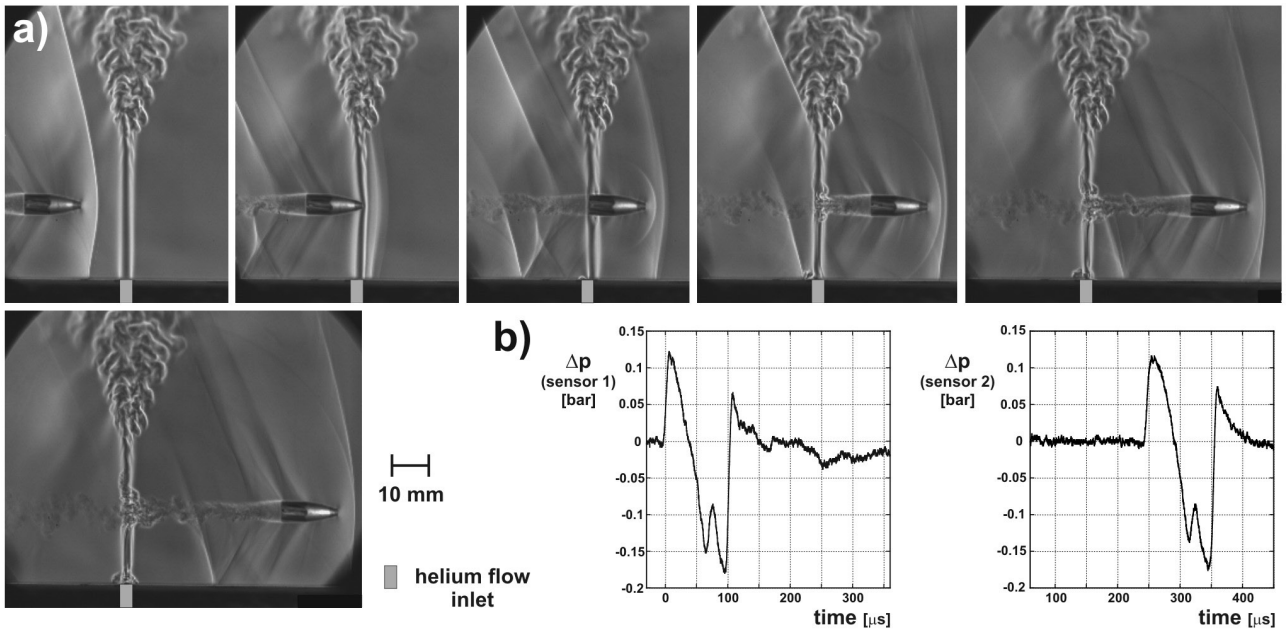

Fig. 6: Interaction of a bow shock generated by a M 1.06 projectile with a helium column (from [16])
a) frames from a time-resolved schlieren visualization taken with 250,000 fps, time between frames 40 μs; the gas inlet is marked in each frame; front lighting was used to provide more details of the shape of the projectile and thus the origin of some of the waves observed around it
b) pressure traces 30 mm upstream and 30 mm downstream of the helium column

While these tests have not explored the full spectrum of the interaction of transonic projectiles with a gaseous column, the results appear to indicate that the influence of this interaction is rather mild and – probably more importantly – only short-lived, so that it appears unlikely that the intended goal of extinguishing a fire by means of high-speed aircraft in ground effect can be accomplished.

TIME-RESOLVED IMAGING FOR EDUCATIONAL PURPOSES

Explaining complex gasdynamic processes to students and/or laypersons, or simply proving that invisible flows are often behind phenomena observed in the world around us can be a challenging task. Flow visualizations greatly facilitate these explanations, in particular time-resolved records that display a process in animated fashion. One potential drawback is that the visualizations may often have an abstract character and may therefore appear to depict an object somewhat detached from the real world that surrounds us. Front lighting, which can be used with all of the presented techniques, and which was already introduced in the earlier example shown in Fig. 6, can help to make the visualization records more accessible, as the record then contains a "normal" image of an object (typically the model immersed in the flow) together with the image of the flow. The full-size schlieren records obtained at the Penn State University [8] are arguably among the most striking examples of such visualizations.

While each shadowgraph, schlieren or interferometry system presented here allows one to obtain, via front lighting, a "normal" image of the object in the visible test section, the coincident schlieren system [8] offers an attractive extension of this approach. In this setup, the imaging lens in front of the camera can image the objects within the test area (the field of view of the schlieren system) as well as objects next to the test area, but outside the visualizing schlieren beam. By choosing an adequate imaging lens, one can obtain a record of an area that may be considerably larger than the field of view provided by the size of the optical system, i.e., the diameter of the mirror. This allows one to obtain an image, in a single record, of objects surrounding the field of view as well as of the flow made visible within the field of view. Time-resolved imaging then allows one to either let objects pass from the surrounding environment into the field of view (thus revealing the flow patterns associated with them) or to turn the visualization system on or off to vividly demonstrate the difference between looking at a process with the naked eye and subsequently through the "eyes" of a visualization system. Both approaches are illustrated in Fig. 7. In Fig. 7a, the first frame shows a rifle bullet flying against a normal backdrop. The associated movie clearly depicts the motion and one can make out signs of the rotation of the bullet. Once the bullet has entered the field of view of the schlieren system, the complex wave pattern around it becomes visible, with the bow shock, the recompression shock and the turbulent wake as main features.

Figure 7b shows the author's daughter observing a table tennis ball suspended on a gaseous jet. The first frame is the normal view that would present itself to any observer in the room – the girl herself may sense the presence of the gas flow but she also only sees the floating ball. When the visualization system is switched on, the flow responsible for keeping the ball afloat becomes visible, and the record clearly shows the structured and laminar flow underneath the ball that detaches and becomes a turbulent wake flow past the equator of the ball.

Both sequences clearly show the presence of normally invisible yet significant flow features in processes that almost everyone can relate to.

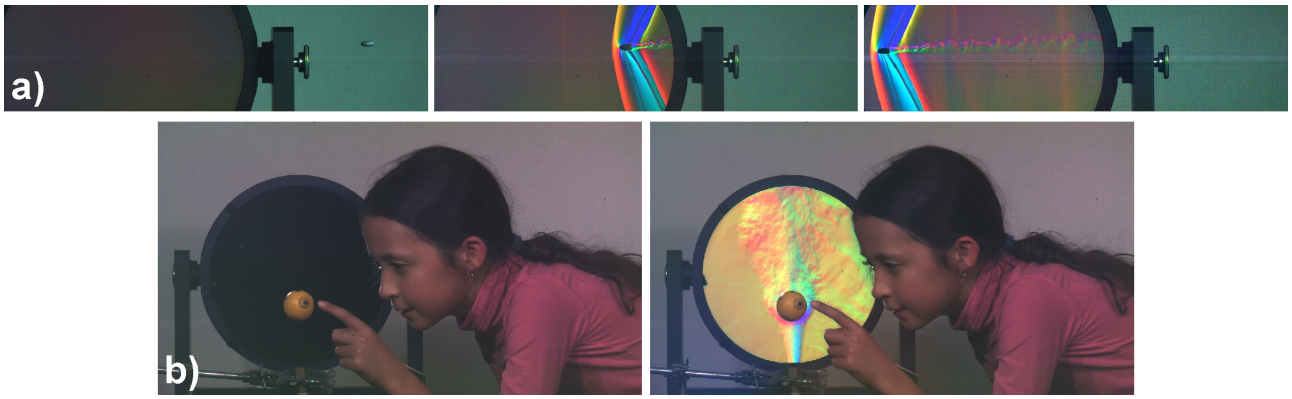

Fig. 7: Time-resolved images obtained with a coincident schlieren system (direction-indicating color schlieren), in which the area surrounding the schlieren field of view is simultaneously imaged.
a) a 0.22 calibre projectile flying with 364 m/s (M = 1.06); three frames of a sequence taken with 40,000 fps, time between frames: 200 µs;
b) gas flow around a floating ball made visible; two consecutive frames of a sequence taken with 60 fps

SUMMARY AND CONCLUSIONS

This paper has presented some applications of time-resolved density-sensitive visualization of compressible flows. Examples for each major set of visualization technique were presented, each of which could demonstrate one of the advantages that true time-resolved visualization provides. In most cases, these advantages outweigh the inherent drawbacks of time-resolved imaging, primarily an inevitable loss of image resolution and quality. Further important scope for time-resolved imaging lies in applications for educational purposes.

ACKNOWLEDGEMENTS

I gratefully acknowledge the contributions of Prof. T. Goji Etoh (Kinki University, Japan), Prof. Beric Skews (University of the Witwatersrand, South Africa), em. Prof. John Dewey (University of Victoria, Canada), Prof. Kazuyoshi Takayama (Tohoku University, Japan) and Prof. Herbert Olivier (RWTH Aachen, Germany) without whom much of the work that provided the basis for this paper would not have been possible. I am also deeply indebted to em. Prof. Hans Grönig (RWTH Aachen, Germany), who introduced me to the exciting field of compressible flows and their visualization. Furthermore, much inspiration for the presented work has come from continuous discussions with Prof. Gary Settles (Penn State University, USA). I would also like to thank my colleague Heath Pratt and my student Vikram Sridhar for their assistance with some of the results presented in this paper. Last, but not least, I would like to express my thanks for the excellent technical support I have received over the last years from members of the SEIT Mechanical Workshop, in particular from Stuart Gay and Michael Jones.

References

1. Merzkirch W. *Flow Visualization, 2nd ed.* Academic, Orlando, 1987
2. Ray S.F. *Scientific Photography and Applied Imaging,* Focal Press, Oxford, 1999
3. Talbot W.H.F. *On the production of instantaneous photographic images,* Phil. Mag. **3**, pp. 73-77, 1852
4. Kleine H. *Filming the invisible – time-resolved visualization of compressible flows*, Eur. Phys. J. Special Topics **182**, pp. 3-34, 2010
5. Ray S.F. (ed.) *High-Speed Photography and Photonics*, Focal Press, Oxford, 1997
6. Etoh T.G., Poggemann D. et al. *A CCD image sensor of 1 Mframes/s for continuous image capturing of 103 frames*, Tech. Dig. Int. Solid State Circuits Conf., IEEE 0-7803-7335-9/02, pp. 45-48, 2002
7. Thoroddsen S.T., Etoh T.G., Takehara K. *High-Speed Imaging of Drops and Bubbles*, Ann. Rev. Fluid Mech. **40**, pp. 257-285, 2008

8. Settles G.S. *Schlieren and Shadowgraph Techniques*, Springer, Heidelberg, New York, 2001
9. Kleine H. *Flow Visualization*, in: *Handbook of Shock Waves* **1**, Academic, San Diego, pp. 683-740, 2001
10. Kleine H. *Time-resolved density-sensitive flow visualization*, DVD, ISBN 978-0-7317-0382-1, UNSW Canberra, 2009
11. Schardin H. *Untersuchung instationärer gasdynamischer Vorgänge als Beispiel für den zweckmässigen Einsatz der Hochfrequenzkinematographie*, Proc. VII. Int. Kongr. Kurzzeitphotographie, Helwich, Darmstadt, pp. 17-23, 1967
12. Kleine H., Dewey J.M., Ohashi K., Mizukaki T., Takayama K. *Studies on the TNT equivalence of silver azide charges*, Shock Waves **13**, pp. 123-138, 2003
13. Svingala F.R., Hargather M.J., Settles G.S. *Modern Optical Methods For Determining the Shock Hugoniot of Transparent Solids*, Proc. 28th Int. Symp. Shock Waves, paper 2749, 2011
14. Moon S.J., Gai S.L., Kleine H., Neely A.J. *Supersonic flow over straight shallow cavities including leading and trailing edge modifications*, AIAA 2010-4687, 2010
15. Kleine H., Olivier H., Tsuji K., Etoh K., Takehara K., Etoh T.G. *Time-resolved Mach-Zehnder interferometry of shock waves*, Proc. 28th Int. Symp. Shock Waves, paper 2495, 2011
16. Kleine H., Oakes B., Pratt H., Neely A., Barber T. *Shock wave interaction with gaseous plumes and flames*, Proc. 29th Int. Congr. High-Speed Imaging & Photonics, paper C-04, 2011
17. Kleine H., Young J., Oakes B., Hiraki K., Kusano H., Inatani Y. *Aerodynamic ground effect for transonic projectiles*, Proc. 28th Int. Symp. Shock Waves, paper 2497, 2011